



**HAL**  
open science

# Study of Rayleigh waves interaction with a spherical ball in contact with a plane surface for the development of new NDT method for ball bearings

Aziz Bouzzit, Loïc Martinez, Andres Arciniegas, Salah-Eddine Hebaz, Nicolas Wilkie-Chancellor

## ► To cite this version:

Aziz Bouzzit, Loïc Martinez, Andres Arciniegas, Salah-Eddine Hebaz, Nicolas Wilkie-Chancellor. Study of Rayleigh waves interaction with a spherical ball in contact with a plane surface for the development of new NDT method for ball bearings. *Ultrasonics*, 2024, 136, pp.107156. 10.1016/j.ultras.2023.107156 . hal-04346510

**HAL Id: hal-04346510**

**<https://hal.science/hal-04346510>**

Submitted on 12 Apr 2024

**HAL** is a multi-disciplinary open access archive for the deposit and dissemination of scientific research documents, whether they are published or not. The documents may come from teaching and research institutions in France or abroad, or from public or private research centers.

L'archive ouverte pluridisciplinaire **HAL**, est destinée au dépôt et à la diffusion de documents scientifiques de niveau recherche, publiés ou non, émanant des établissements d'enseignement et de recherche français ou étrangers, des laboratoires publics ou privés.

# Study of Rayleigh waves interaction with a spherical ball in contact with a plane surface for the development of new NDT method for Ball bearings

Aziz Bouzzit <sup>\*a</sup>, Loïc Martinez <sup>a</sup>, Andres Arciniegas <sup>a</sup>, Salah-Eddine Hebaz <sup>a</sup>, Nicolas Wilkie Chancellier <sup>a</sup>,

<sup>a</sup> Laboratoire SATIE (UMR CNRS 8029), CY Cergy-Paris Université, 5 mail Gay Lussac, 95031 Neuville Sur Oise, France  
Corresponding author: \*aziz.bouzzit@cyu.fr

## Abstract

Surface Acoustic Waves (SAW) such as Rayleigh waves have a low attenuation property that makes them suitable for non-destructive testing (NDT) of large surface areas. The investigation methods are focused on material properties estimation and crack localization on canonical geometries (plane, sphere, cylinder).

In some situations, the object under investigation is not directly accessible, such as the spherical steel ball in ball bearings, in which case information can be extracted indirectly by studying the interaction between the SAW and the object under investigation. Therefore, in order to measure the properties of a ball in a ball bearing, one has to study firstly the interactions of Rayleigh waves at the sphere-plane interfaces.

As ball bearing can be seen as a repetitive assembly of spherical objects in contact with plane surfaces, the goal of this paper is to present an experimental and numerical study of the interaction between a SAW propagating on the surface of an aluminum block with a solid sphere, mainly a steel ball, like the ones found in ball bearings. This study focuses on the complete characterization of the SAW generated on the steel sphere by the direct Rayleigh waves and the waves generated after their interaction with the sphere. The latter are propagated from the sphere back to the surface of the aluminum block.

The aim of this study is to visualize the different waves involved in the interaction, which highlighted the existence of back generated waves : on one hand, using Gabor analysis, it was shown that the back generated waves are of the same type as the direct wave, and on the other hand, using dispersion curves, it was shown that the SAW are dispersive on the surface of the steel sphere. The different modes can be distinguished and the back generated waves contain information related to the steel sphere these last can be extracted either by using a spatiotemporal signal or a single point time signal.

On one hand, the experimental study is accomplished on a steel sphere with a radius of 6 mm. The waves are generated on a 20x12.5x10 cm<sup>3</sup> aluminum block using a 1 MHz Panametrics shear wave contact transducer. This block is considered as infinite medium at operating wavelengths. The normal displacement on the surface of the sphere and the block are measured using a Laser vibrometer. On the other hand, a numerical study is performed using a three-dimensional time-domain finite element model. The obtained results show that characterization of material properties of the sphere is possible through the generated waves on the surface of the block.

**Keywords:** *Surface waves, Steel sphere, ball bearings, Laser Vibrometer, Finite Element Method.*

## **1. Introduction**

Historically, the vibration of homogeneous elastic spheres was firstly studied by Horace Lamb in 1881 [1]. In fact, in geophysics, it constitutes the simplest model of the Earth when studying seismic waves [2]. However, the curved nature of its geometry makes it difficult to extract point-like signals at the surface of relatively small, millimeter scale, spheres. The apparition of non-contact optical techniques such as laser vibrometry made it possible to scan compact curved

surfaces, and thus allowing us to study waves propagating on such spherical elastic objects and to develop new methods related to NDT of balls.

In literature, using an optical heterodyne interferometer to detect vibrational signals and a laser source as a wave generator, it was shown that the dispersive nature of SAW on the sphere is the result of its curvature [3]. Other works present a multiple synchronized laser point-sources arranged in a line on the sphere, which generates a SAW propagating along the circumference following the direction perpendicular to the line source without beam spreading due to diffraction [4]. This feature was exploited to develop a high-precision NDT method dedicated to the characterization of the surface of solid spheres of a ball bearing, by utilizing the important number of round trips of a high frequency stable surface wave [5].

The theoretical and experimental investigation of the stable properties of a SAW generated by a line source was presented by Clorennec and Royer [6]. In addition, the geometric conditions needed to generate a propagating collimated spherical beam are highlighted.

In 2007, Yamanaka developed a sensor integrated on the surface of the steel sphere, using the collimated nature of the beams. The sensor helps to understand the physics of SAW propagation and its interaction with a fluid surrounding the ball [7]. Similarly, in a previous work, we have studied the interaction between a fluid sphere (droplet) and a solid plane, using 3D Gabor analysis in order to identify the shape, wavelength, frequency, attenuation, group velocity and the full conversion sequence along propagation of the wavefront [8].

Royer proposed a theoretical formulation of the dispersive behavior of SAW in spheres and cylinders: an equation with two dimensionless coefficients, which can be obtained from the asymptotic behavior of the phase and group velocities at high frequency [9].

The first real time 2D imaging of SAW on a solid sphere was carried out by Otsuka et al. [10] using an ultrafast interferometric optical technique. Fourier analysis was performed to estimate the wave velocity and the source function governing the propagation through the poles. When using a point source, the propagating SAW converges to the pole opposite to the generation point and the convergence area properties changes as function of the frequency of the excitation [11]. In the case of SAW on hollow spherical shell, an analytical model is proposed by Ma et al. and validated using simulation and experiment based on laser ultrasonic technique [12].

Aforementioned research was focused on the study of SAW propagation on a solid sphere, independently of the overall system. In this study, we propose to characterize the interaction of SAW propagating at the plane surface of a solid block with a solid sphere on top. It would be the first step towards the development of a characterization method of ball bearing as a complete structure without the need to disassemble it. In fact, the geometry of a ball bearing may seem to be intricate, since multiple spheres are in contact with two circular rings. Because of that, one can imagine that the propagation of acoustic waves on such geometry will be complicated. The idea to simplify this problem is to consider a ball bearing as a periodic structure made of a geometric unit, namely: a steel sphere in contact with plane surfaces. Consequently, the starting point to understand the complex behavior of SAW propagating on a ball bearing is to study the interaction between a SAW on a solid plane in contact with a solid sphere.

In this paper, an experimental setup and a numerical model, are used to extract time signals of propagating waves, on top of the solid sphere and the area surrounding it . The extracted time signals allow the analysis of the different waves involved in the interaction and their evolution over time.

The analysis of the spatiotemporal signals extracted on the surface of the sphere will complete the work of Otsuka et al. [10] related to the understanding of the vibrational modes of the steel sphere. The understanding of this interaction is the key to develop a NDT method for ball bearings. The main idea is to generate a SAW that will propagate around the outer-ring of the ball bearing and interact with all the steel spheres. The extraction of signals at the outer-ring should give us information, not only about its condition but also on all of the steel spheres and the inner-ring.

This paper is organized in three parts. The first section is dedicated to the experimental setup, the numerical model and signal processing techniques deployed to characterize the wave propagation. In the second section, the obtained results are shown and examined in light of those found in the literature. Finally, a discussion that summarizes the main findings of this study and its importance for future developments is given in the last section.

## **2 Materials and methods**

### **2.1 Protocol**

The experimental and numerical studies of the SAW propagation and its interaction with a solid sphere on a plane surface are conducted in three steps.

The first one consists on visualizing and analyzing the time series extracted from the experimental setup and the numerical model. The aim is to characterize the generated Rayleigh wave on the block, the SAW on the sphere and the waves generated from the sphere to the block. Since the experimental signals correspond mainly to the normal displacement, the numerical data will allow us to fully analyze the three components of the displacement field of these generated waves, in order to identify their nature.

The second step consists of analyzing the results obtained from the 3D Gabor analysis. The latter enables the validation and quantification of the information found in the first step. This consists of comparing the frequency and wavenumber contained in each type of waves, as well as monitoring their evolution during the transition from the direct waves to the back-generated waves. The wavefront of each wave can be quantified by local wavevectors as they are normal to it.

In the third step, various dispersion curves are calculated from experimental and numerical data. They are used to analyze the SAW propagating on the sphere with the generated waves on the surface of the block. On the one hand, an approximation based on the circum-navigation along the meridian is applied to estimate the group velocity dispersion curve [9]. The results are obtained from a signal at the pole of the sphere and at a single point on the block in the surrounding area. On the other hand, a classical 2D Fourier Transform analysis is carried out to compute the dispersion curves from a set of signals extracted from aligned points on the top of the sphere and on the surface of the block following the propagation axis. The goal is to analyze the modal content of the propagating waves and to compare it to theoretical curves. The comparison also allows a clear validation of the numerical model.

## **2.2 Experimental setup**

To study the interaction between SAW and a solid sphere, a steel ball (radius  $r = 6$  mm) extracted from a ball bearing is mounted on the top of an aluminum block as a support for the SAW. Its generation is achieved using a 1 MHz (Panametrics) shear wave contact transducer ( $\varnothing = 1$  inch) excited by a pulse generator (JSR Ultrasonics DPR300). The transducer is positioned near the edge and on the side of the block, to ensure a Rayleigh wave excitation, as shown in Figure (1). Measurement of normal displacements is carried out by single-point Laser vibrometer (OFV-505 Polytec) and its associated controller (OFV-2570). The Laser head is placed horizontally on

anti-vibration optical table and the beam is pointed perpendicularly to the top surface of the block using a mirror of 45°. The block is mounted on a 2D Motorized linear stage to control the scanning point.

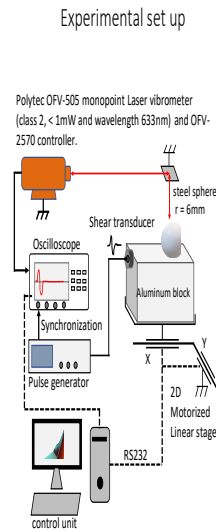


*Figure 1: Experimental setup for measurement of normal displacements.*

The scan is conducted over a 2D grid surface ( $S = 2.5 \times 2.5 \text{ mm}^2$ ) including the solid sphere and the surface of the block surrounding it. This method will allow us to detect and study the direct wave propagation from the block's surface to the sphere and the waves generated from it. For each spatial point of the grid, the time signal and the position are acquired through an oscilloscope. The grid-points are spaced by  $dx = 0.2 \text{ mm}$  and  $dy = 0.2 \text{ mm}$ . The acquisition protocol and signal post-processing were implemented using MATLAB software.

### 2.3 Numerical Model

The experimental setup enables the detection of the normal displacement at each scanned point. However, in order to perform a complete characterization of the vibrational behavior, the three

components of the displacement field are needed. A 3D numerical time-domain finite element model is then developed in the following, mimicking the experimental conditions using a commercial software. The geometry is illustrated in Figure (2).

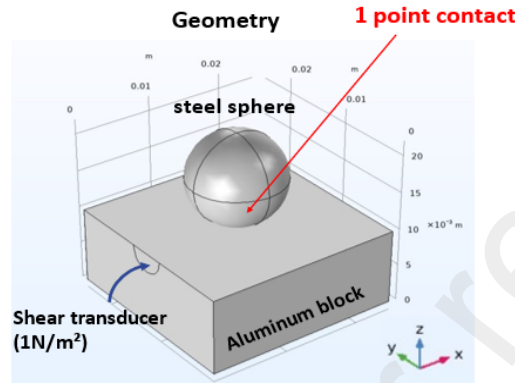


Figure 2: Numerical model geometry and configuration.

The steel sphere is modeled on top of the aluminum block, with dimensions  $2.5 \times 2.5 \times 1 \text{ cm}^3$ , and the contact condition between the two geometries is chosen to be a single point. Because the dimensions of the block cannot be considered as infinite at the investigated wavelength, the block's boundaries are free and with low reflection in order to approximate this condition. For the sake of simplicity, the shear wave transducer is simulated by a surface force acting in the Z direction, with magnitude of  $1 \text{ N/m}^2$  corresponding to the typical magnitude of the pressure generated by transducers [13,14]. The excitation signal is a burst of 5 sinusoidal cycles on central frequency  $f_{ex} = 1 \text{ MHz}$ . Table (1) gathers the elastic properties of the aluminum and steel used in the block and sphere respectively.

Table 1. Elastic properties of Aluminum and steel

	<i>Aluminum (block)</i>	<i>Steel (sphere)</i>
<i>Young's modulus (E)</i>	69 GPa	200 GPa
<i>Poisson coefficient (ν)</i>	0.33	0.30
<i>Density (ρ)</i>	2730 kg/m <sup>3</sup>	7850 kg/m <sup>3</sup>
<i>Shear wave velocity (c<sub>T</sub>)</i>	3082 m/s	3130 m/s
<i>Longitudinal wave velocity (c<sub>L</sub>)</i>	6119 m/s	5856 m/s

The block and the sphere are discretized using linear three-dimensional tetrahedron-shaped elements. The stability of the integration scheme depends on the spatio-temporal discretization. In order to meet the recommended minimum requirements, the maximum size of an element is set at  $L_{Max} = c_{T_{Al}} / (10 \cdot f_{ex}) = 0.3$  mm with a time increment  $dt = L_{Max} / c_{L_{Al}} = 0.049$  μs, where  $c_{T_{Al}}$  and  $c_{L_{Al}}$  are the shear and longitudinal wave velocities in Aluminium.

The three components of the displacement field ( $u_x, u_y, u_z$ ) are extracted in two different point, the first one on the top of the sphere, with the coordinates (1.25 cm, 1.25 cm, 2.2 cm), in order to estimate the group velocity of Rayleigh wave as mentioned in the third step of the protocol, and the second one on the surface of the block with the coordinates (1.875cm, 1.25cm, 1cm), this last will be used in the identification of the waves generated by the sphere as explained in the first part of the protocol. The extracted signals are post-processed by MATLAB software.

## 2.4 Wave characterization methods

Firstly, the measured vibrational signals are organized in order to have a 2D spatio-temporal representation of the wave propagation. In this step, a qualitative information can be observed about the wavefront and the directivity of different types of waves.

Secondly, the study is focused on analyzing the frequency and wavenumber content of each detected wave, and how some key characteristics can be extracted from these properties, such as the group and phase velocities of each of the materials (steel and aluminum). This allows us also to validate the qualitative information of the first step and to establish the links between the different types of detected waves. Starting from the measured displacements  $(u_x, u_y, u_z)$ , Gabor analysis is performed to determine wavevectors  $(k_x, k_y)$ , for each frequency  $f$  and time instant  $t_i$ . Respecting space-wavenumber and time-frequency dualities [8], equation (1) is a summary of the input and output parameters of Gabor Transform.

$$s(x, y, t) \xrightarrow{\text{Gabor}} S(x, y, t, k_x, k_y, f), \quad (1)$$

The numerical implementation of Gabor transform may be computationally very expensive depending on the size of the data. However, it is possible to analyze the wavenumbers propagating over a line. In order to achieve this approach, time signals received at a series of equally spaced points along the path can be extracted and organized as a spatio-temporal matrix (2D image). Dispersion curves can be determined by applying two-dimensional Fast Fourier Transform (2D FFT) on the spatio-temporal data in order to represent the wavenumbers propagating at each frequency. This method gives access to the wave modes propagating along the path [15], but the time and space localizations are lost due to the Fourier Transform.

Finally, the study of the dispersion curves on the sphere and on the surface of the block gives access to the phase and group velocities of SAW in both materials, and allows to understand that information about material properties of the sphere are transmitted to the surface of the block.

### 3. Results

#### 3.1 Time data

After extracting signals from the experimental setup and performing some post-processing, a cube of data is obtained, containing the time evolution of the normal displacements for all the scanned points. The following figure illustrates the recorded signals at  $t_i = 24 \mu\text{s}$ .

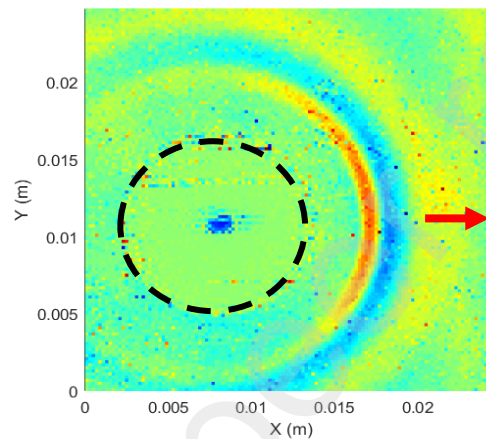


*Figure 3: Circular wave generated by the steel sphere.*

In Figure (3), the dashed black circle highlights the edge of the steel sphere. Circular wave can be seen, centered on the contact point between the sphere and the block, propagating away from the sphere. This information corresponds to the wave transmitted by the sphere to the block after its interaction with the direct Rayleigh wave.

The red arrow indicates the direction of propagation of the direct wave. The generated wave has certain directivity of energy in the line of propagation of the first direct wave, and that the amplitude of the circular wave is higher on axis.

From the 3D numerical model, the three components of displacements can be extracted for each point of the mesh. This data can be organized in 6D hypermatrix. The following 3D representation

illustrates the amplitude of displacements captured at  $t_i = 58 \mu\text{s}$  (Figure (4)), this instant corresponds to appearance of the third generated wave, the reason induced for choosing this wave is because the first one is interfering with the direct wave, as we can see in Figure (5) around 24  $\mu\text{s}$ .

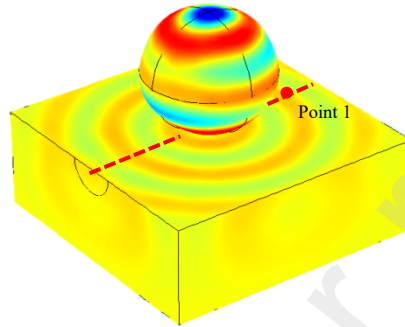


*Figure 4: Circular waves in the numerical model.*

Similarly, as ever observed for the experimental results, the circular wave generated by the sphere are also highlighted. One can clearly see here that the source of the circular waves is located in the contact point between the sphere and the block, the colormap lets us identify the wavefront.

To further investigate the generated waves, the time series of the three components of displacements are shown Figure (5) on a point located in the propagation axis of the direct wave (see the red point in Figure (4)).

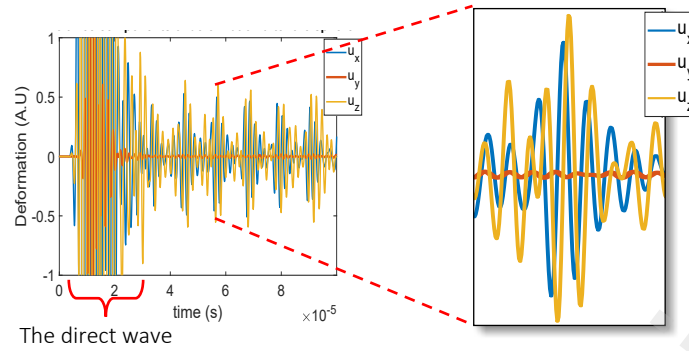


Figure 5: Time series extracted from numerical data.

In the extracted time series, the two types of waves are visualized: the direct wave is the first one to be recorded, the amplitude of this last was saturated in order to be able to observe the generated waves. For each spin of the SAW on the sphere, a wave is generated on the surface of the block and this last is recorded as a pulse in the time series.

If a zoom is done on one of the signals, two important elements can be observed. The first one is the low amplitude of the  $u_y$  component of the generated wave and the second one is the  $90^\circ$  phaseshift between the  $u_x$  and  $u_z$  components. These features are the key characteristics of a Rayleigh wave. Based on these results, a conclusion is done that the generated waves are of Rayleigh type.

### 3.2 3D Gabor analysis

Using the numerical data, the generated waves have been determined as Rayleigh waves, as the direct one. In this part, 3D Gabor analysis [8] is performed in order to distinguish if the two waves have the same properties in terms of frequency and wavenumbers.

The following figure (Figure (6)) illustrates the results of the Gabor analysis applied on the experimental data. Three different time are shown, corresponding to the passage of the direct

Rayleigh wave ( $t_1 = 3.8 \mu\text{s}$ ), the transition from direct wave to the circular wave ( $t_2 = 8.9 \mu\text{s}$ ) and the propagation of circular wave ( $t_3 = 11.7 \mu\text{s}$ ). These snapshots are done for a frequency  $f = 1.4 \text{ MHz}$ , which corresponds to a resonance frequency, for which the wavelength of the propagating waves is in the order of magnitude as the scanned surface. In this figure, the left figures correspond to the displacements propagating at the frequency of 1.4 MHz, the middle figures are the 2D spatial FFT of the displacements and the right figures illustrate the local estimated wavevectors constructed from the estimated wavenumbers in the  $x$  and  $y$  direction.

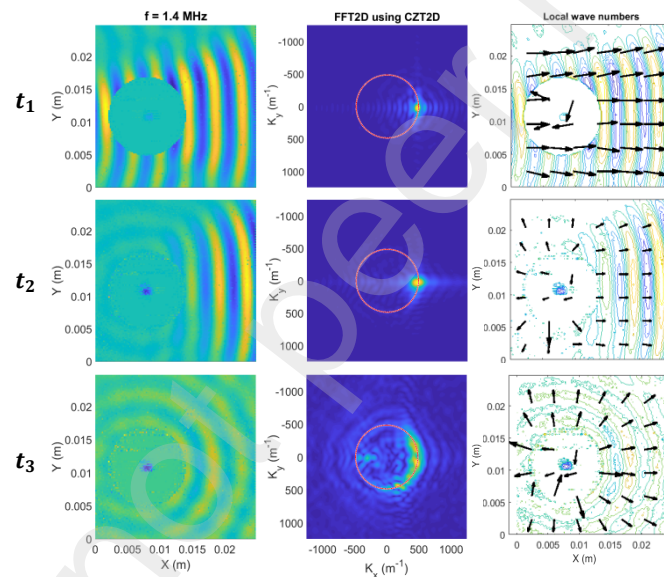


*Figure 6: 3D Gabor analysis results.*

The time instant ( $t_1$ ) shows the direct wave propagating with a plane wavefront in the  $x$  direction, as illustrated by the local wavevectors, the spatial 2D FFT in the middle shows that the propagating wavenumbers are located in the circle corresponding to wavenumbers of Rayleigh waves. Time instant ( $t_2$ ) illustrates the transition from direct to circular waves, the beginning of the appearance of the circular wavefront can be observed, while the propagating wavenumbers remain located on the Rayleigh circle in the spatial 2D FFT plane. In the propagation of the circular wave shown in

time instant ( $t_3$ ), the circular wavefront illustrated by the local wavevectors and all the propagating wavenumbers are shown to be still located in the Rayleigh circle. The directivity in the  $x$  direction is validated by the high amplitude of the positive  $k_x$ . The results are in good agreement with the information recovered from the visual inspection of the time signal data. One can conclude that direct wave and the generated waves are of the same nature.

### **3.3 The dispersive behavior of waves**

It has ever been shown that the propagation of SAW in solid sphere is dispersive [3]. From the time signal extracted on top of the sphere, the dispersive nature of wave can be observed and the group velocity of the SAW can be estimated [9]. In this part, the previously developed theory is applied in the studied case: firstly on a single point time signal extracted from the top of the sphere and on the surface of the block, secondly on a spatio-temporal signals extracted on the same place as aforementioned.

#### **3.3.1 Single point time signal analysis**

One signal is extracted from the top of the sphere, in both experimental and numerical cases. The signals are represented in time and frequency domains (Figure (7)).

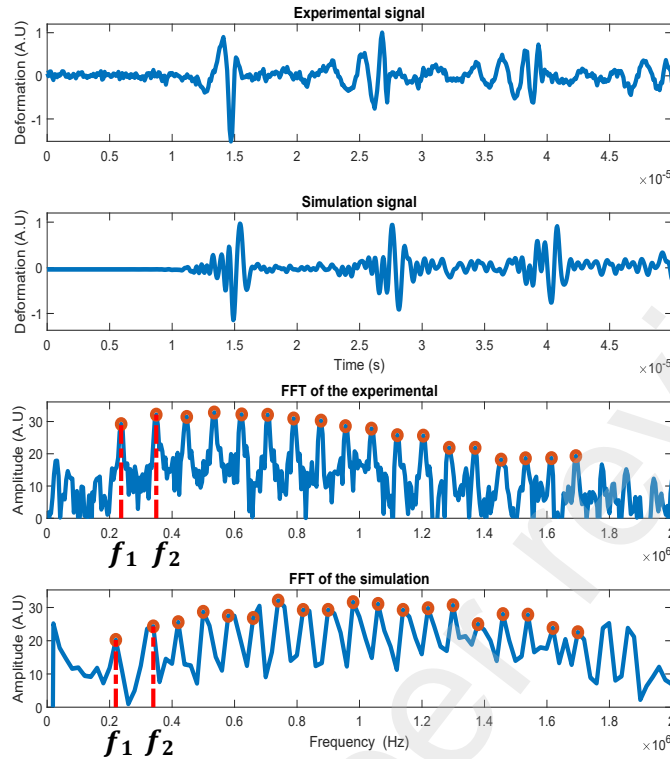


Figure 7: Time and frequency representations of signal extracted from the top of the sphere.

The extracted time series is periodic for both the experimental and numerical cases. A peak in the amplitude is detected each time the SAW does a spin over the sphere. In the frequency domain, the periodicity is represented by the line (peak) nature of the spectrum.

An amplitude spectrum technique for the measurement of phase and group velocities of dispersive waves in solids can be used from the resonant frequencies corresponding to vibrations modes [16,17]. These modes, or mechanical resonances, depend on the shape of the objects. In our case, successive periodic waves are observed during the interaction of a SAW with the sphere. From this phenomenon, the obtained signals are similar to those of resonance scattering such as the Regge modes observed in nuclear physics [18].

Therefore, the group velocity of the surface wave can be estimated from the spectrums by means of the following formula [9]:

$$V_R = 2\pi r \Delta f, \quad (2)$$

where  $r$  is the radius of the ball and  $\Delta f = (f_{n+1} - f_n)$  is the difference between two successive frequency peaks of the line spectrum (Figure (7.b)).

Equation (2) estimates the mean group velocity over the range of frequency between two successive modes. Figure (8) shows the values velocity as function of the mean frequency between two successive modes used in the estimation.

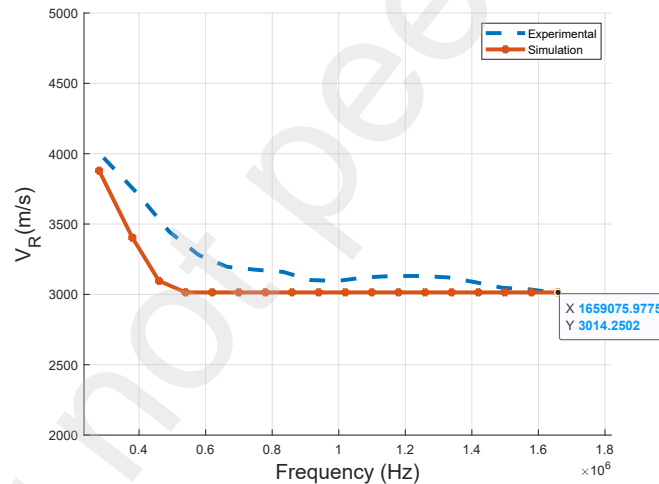
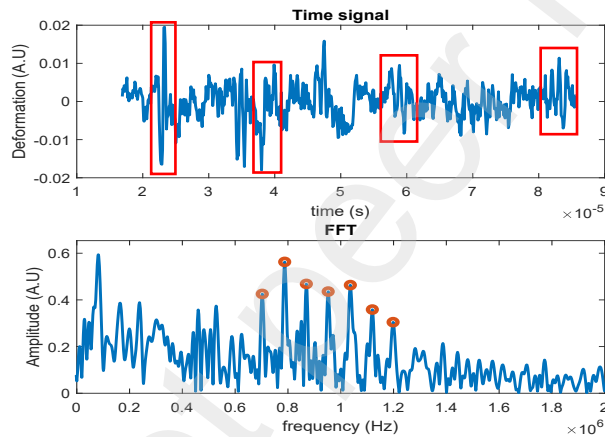


Figure 8: Estimation of Rayleigh wave group velocity on top of the sphere.

The estimated values, in both experimental and numerical cases, are ranging between  $3000 \text{ m.s}^{-1}$  and  $4000 \text{ m.s}^{-1}$ . The figure shows that velocity decreases as the mean frequency increases, converging to the value of  $V_{R_{estim}} = 3014 \text{ m.s}^{-1}$  (asymptotic behavior beyond the 15<sup>th</sup> mode). This value of the group velocity of Rayleigh waves is in a good agreement with the literature ( $V_{R_{lite}} = 2960 \text{ m.s}^{-1}$ , [9]), with less than 2 % error.

This technique is very efficient, it only needs one signal extracted from the top of the sphere to estimate the group velocity of SAW, it takes advantage on the geometry of the sphere where extracting a signal from one point is equivalent to having multiple extraction points equally distanced with a distance  $2\pi r$ .

Likewise a single time signal is extracted on the surface of the block, this last will undergo the same post-processing as the signal extracted on top of the sphere. The following figure illustrates the extracted signal and its corresponding FFT :



*Figure 9: Time and frequency representations of signal extracted from the surface of the block.*

In Figure (9) the noise in the time signals made it difficult to see different generated waves, but in the frequency domain, the line spectrums corresponding to different modes can be well detected. Using Equation (2), their group velocity can be estimated, as illustrated in the following figure:

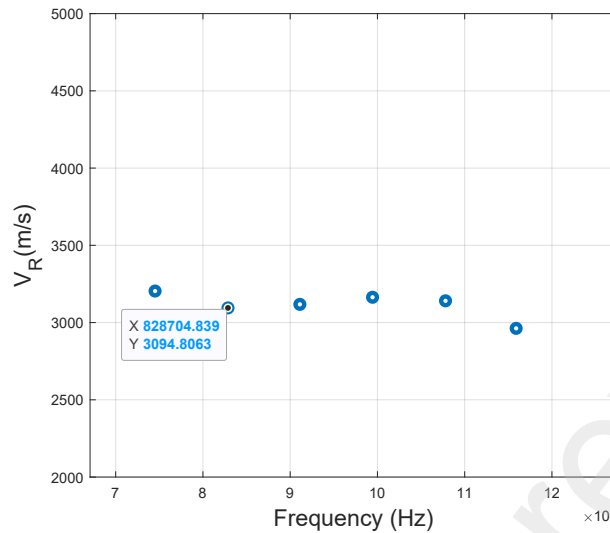


Figure 10: Estimation of Rayleigh wave group velocity on the surface block.

The estimated group velocity is around  $V_R = 3094 \text{ m s}^{-1}$ , which is in a good agreement with the already found values on the top of the steel sphere (error less than 3 %). This information is related to the material properties of the steel sphere, one were able to measure it on top surface of the aluminum block.

The low quality of the single point time signals made it difficult to detect a large number of well isolated modes, which is the key to a good estimation of the group velocity.

### 3.3.2 Spatio-temporal signals

In the following part, the use of a spatio-temporal approach is investigated as a solution to the problems encountered in the single point time signal case.

Using the 2D FFT technique, Otsuka et al. [10] have extracted the dispersion curves of waves propagating on the sphere. In their results, one can see the overall behavior of the dispersion curves, but the individual modes were not distinguishable due to the space discretization.

By following the same steps, considering the experimental setup mentioned above, 2D data are extracted over a line of points on top of the sphere, as shown in Figure (11).

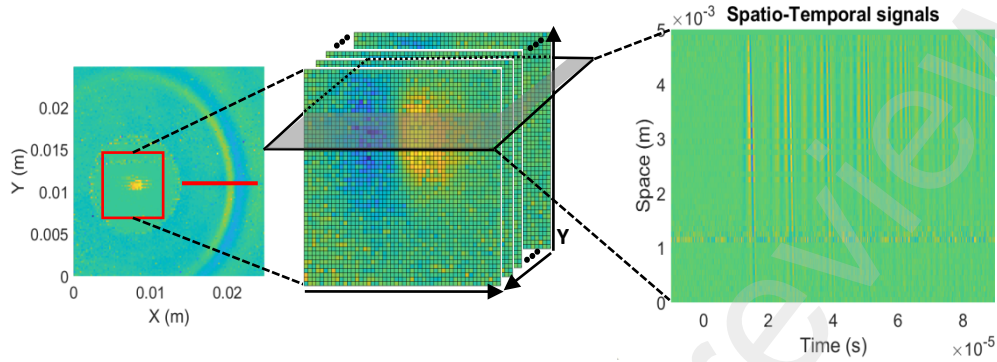


Figure 11: Spatio-temporal signal extraction on top of the sphere.

The 2D FFT signal processing is applied on the spatio-temporal data to obtain the dispersion curves as illustrated in Figure (12.a).

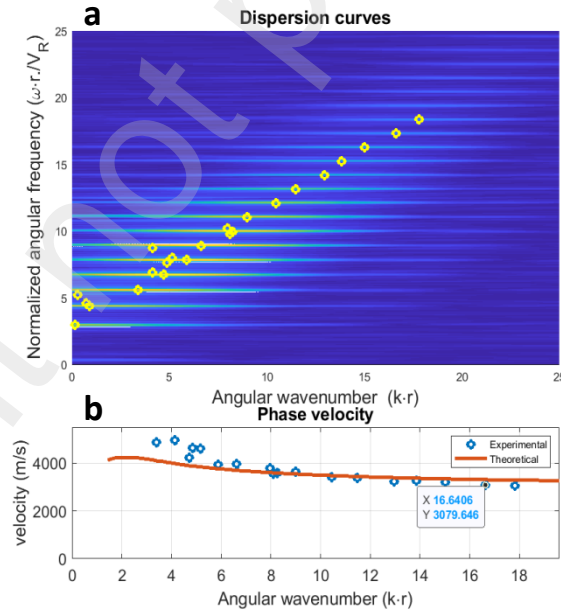


Figure 12: Dispersion curves and phase velocity of modes

In the studied case, the individual Regge modes are distinguishable, due to the fine space discretization ( $dx = 0.2$  mm), where every yellow line represents an individual mode. The frequency and wavenumbers axis are normalized to observe the order of each mode. From the maxima of these modes, indicated by the circles, the discrete phase velocity can be estimated and compared to the theoretical values given by Royer and Clorennec [6]. A good agreement is to be noticed when comparing the value of the measured phase velocity with those estimated by the theoretical expression for the large values of angular wave number.

The low other modes are more dispersive, because of their corresponding wavelengths which are in the order of magnitude of the sphere dimension, the semi-infinite plane domain condition is not satisfied for these wavelengths.

From the discrete peaks (modes), the values of the group velocity can be estimated using Equation (2). The  $\Delta f$  are extracted from the difference in frequency between two observed modes in the dispersion curves. The group velocity is plotted as function of the mean frequency between two modes (Figure (13)). The shaded part of the figure corresponds to the low frequency low wavenumber modes, these modes are very dispersive due to their wavelengths close to the dimensions of the ball. Measurements over a great distance and long acquisition duration are needed to properly extract these modes, conditions that cannot be satisfied with the small dimension of the ball. For a frequency of  $f = 500$  kHz the wavelength of Rayleigh waves on steel is  $\lambda = V_R / f = (3014 \text{ m / s}) / (5 \cdot 10^5 \text{ Hz}) = 6.028 \text{ mm}$ , this value corresponds to the radius of the steel ball, below 500kHz the wavelengths are bigger than the radius.

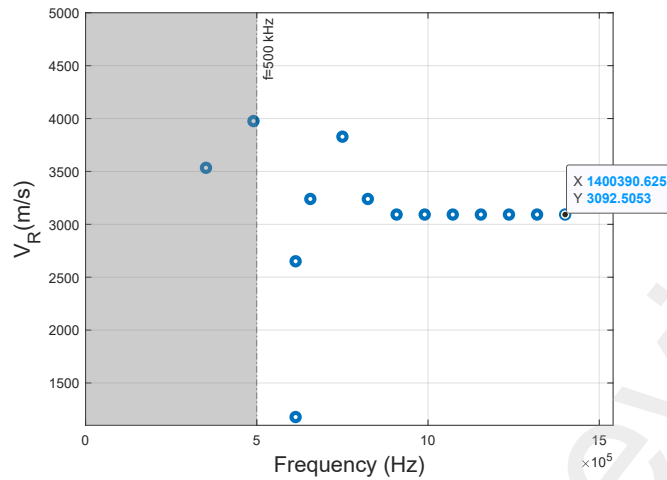


Figure 13: Estimation of the group velocity from 2D signals extracted on top of the sphere.

One more the estimated value is in a good agreement with the ones estimated by the already mentioned methods and the ones found in the literature. In the following, this value is taken as reference to verify whether the estimated values from the times signals on top of the block is correct or not.

As one has already observed that the sphere generates circular waves on the surface of the block after its interaction with the direct waves, these waves are the results of dispersive SAW propagating on the sphere. It is known that the propagation of surface wave on a semi-infinite plane is not dispersive [19]. This is a situation where a dispersive structure (the sphere) is generating waves on a non-dispersive one (the block). The generated waves are non-dispersive, as already shown that they are of Rayleigh type which are not dispersive on a block, but it will be interesting to see if the generated waves conserve information either related to the dispersive nature or the material properties of the sphere.

In the same way, signals are extracted from a line on equally spaced points, the line is located on the propagation axis of the direct wave, the points are extracted after the sphere, as shown by the

red line in Figure (11). From this data, the 2D FFT of a spatio-temporal signal is computed to achieve the dispersion curves (Figure (14)).

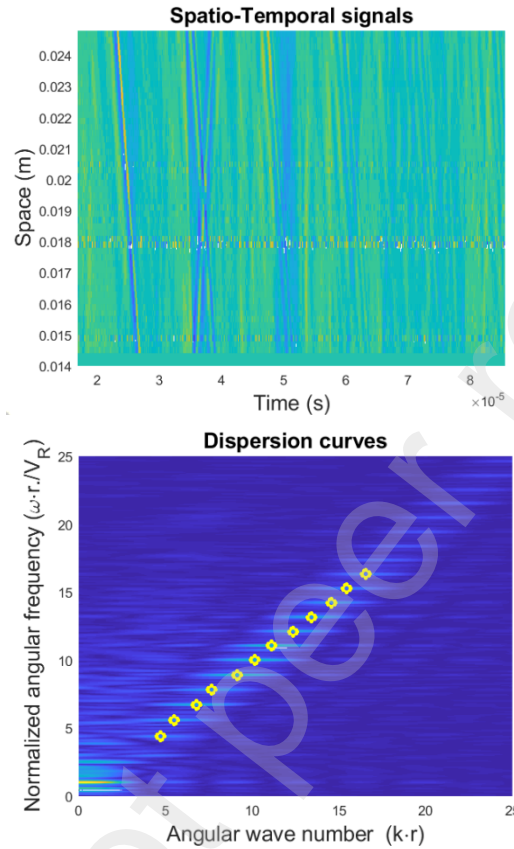


*Figure 14: Spatio-temporal and dispersion curves of signal extracted on top of the block.*

The obtained dispersion curve is of the same nature as the one observed on top of the sphere, with the difference of the individual modes (peaks) being localized in the line of the wavenumbers and frequencies corresponding to the Rayleigh waves in aluminum. The discretized nature is related to the periodic signals generated by the sphere, this aspect contains information about the steel sphere.

To verify that the peaks are located in the line of Rayleigh waves, the phase velocity is calculated from the values of wavenumbers and frequencies of each peak as shown in Figure (15).

In this representation, the values of the phase velocity can be observed constant as function of the angular wavenumber, which means that the propagation on the block is not dispersive. The value of the phase velocity is  $V = 2915 \text{ m.s}^{-1}$  which is in a good agreement with the values of Rayleigh waves phase velocity in aluminum found in the literature ( $V_{R_{Al}} = 2930 \text{ m.s}^{-1}$ , [9]), with an error less than 1 %.

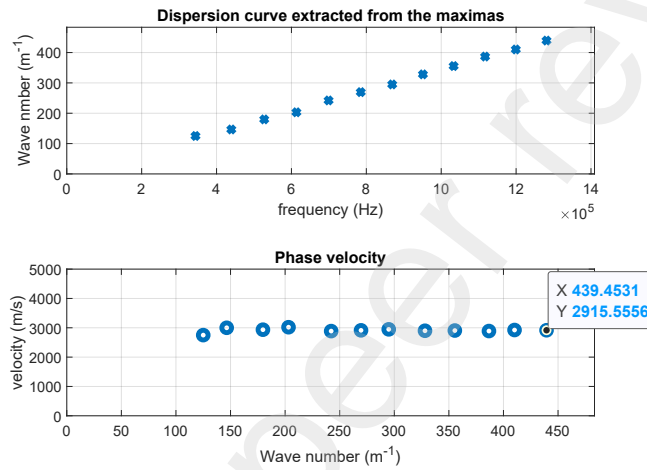


Figure 15 : Estimation of the phase velocity on the aluminum block.

In Figure (15), the advantage of using a spatio-temporal signal rather than a single time signal can be noted, the number of detected modes is way larger than the first case, this means that a good estimation of the group velocity is obtained by utilizing equation (1) in the same manner. The following figure (Figure (16)) represents the estimated group velocity from the difference in frequency between the different modes:

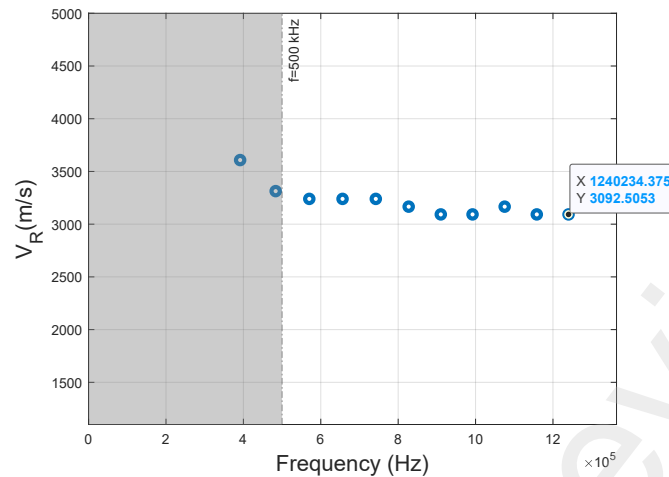


Figure 16: Estimation of the group velocity from 2D singles extracted on top of the block.

The estimated group velocity converges to the values of  $V_{RSteel} = 3092 \text{ ms}^{-1}$ , this value corresponds to the one of Rayleigh wave in the steel sphere, as we estimated before (Figure (13)). This measurement is an information related to the original source of the circular waves, the steel sphere, the information is transmitted to the block, and can be accessed without the need of a direct measurement on the steel sphere. As in Figure (13), the shaded part corresponds to the very high dispersive wavelengths close the dimensions of the ball.

This result is of great importance, as it will be building block on which the NDT method will be constructed, as an important material related parameter (Rayleigh wave velocity). Consequently, the material properties of balls can be measured without the need to take them out from the ball bearing.

#### 4. Discussion

In this paper, experimental and numerical studies are performed in order to understand the interaction of a SAW with a solid sphere and the nature of the waves generated at the surface of

the block. After interaction between the direct wave and the sphere, the results concluded that the successive transmitted waves towards the block conserve the waveform of the SAW propagating on the sphere. This allows us to deduce the dispersive behavior of the waves propagating on the sphere and to extract material related properties as Rayleigh waves group velocity, only studying the transmitted waves towards the block.

In order to achieve that, two types of signals were used to measure the same quantity (Rayleigh waves group velocity), single and spatio-temporal signals extracted from the top of the sphere and on the surface of the block. The two signals have undergone through relatively the same post-processing, involving Equation (2) as the main tool to estimate the group velocity. The results are summarized in Table (2).

*Table 2 : Estimated Rayleigh group velocities in different cases.*

	Measured on top of the sphere		Measured on the aluminum block	
	Single point signal	Spatio-temporal signal	Single point signal	Spatio-temporal signal
<b>Rayleigh Group velocity (m/s)</b>	<b>3014</b>	<b>3092</b>	<b>3094</b>	<b>3092</b>

As already mentioned above, the obtained results are in a good agreement with the values found in the literature. Hereby, this work is focused on the difference between the measurements on top of the sphere and on the block in both cases. One can see that a difference is noticeable between the values estimated using single point signal, this is due to the low quality of the time series extracted on the surface of the sphere. The latter was not the case for the spatio-temporal signal, for which the same value is found in both the top of the sphere and on the surface of the block. The phase velocity has not been used to validate the information extracted on the surface of the

block, as the measurement of this last is only possible via the spatio-temporal signals extracted on top of the sphere. However, the values and the variation of the phase velocity were used to validate the results as shown in Figure (12).

In the single point signal case, the discrepancy is still relatively very small, around 2.6% relative error. This error can be accepted considering the time and the materials needed in order to extract a spatio-temporal signal on the surface of the block.

## 5. Conclusion

In this article, the interaction between a direct SAW and a solid steel sphere is studied experimentally and numerically, with the aim of characterizing and visualizing the different waves involved in the interaction, which are the direct wave, the wave transmitted to the sphere and the back generated waves. The analysis of these different waves, especially the back generated ones, allows us to extract material information related to the sphere without the need to make a direct measurement on the sphere.

Using the Gabor analysis and the results of the numerical simulation, the back generated waves are concluded to be of the same type as the direct wave. The dispersion curves calculated from the spatio-temporal signals of the surface of the sphere allowed us to extract and distinguish the different vibrational modes and to compare them with the Regge modes.

To ensure that the information related to the material properties of the sphere can be transmitted to the surface of the block, two types of signals - spatio-temporal and single point time signals - are extracted both on the surface of the sphere and on the block. The two signals undergo the same processing to extract the group velocity of Rayleigh waves, for the two extraction positions. The estimated values are in good agreement with each other and with the values found in the literature.

It can be seen that the discrepancy between the values obtained from the spatio-temporal signals is smaller than in the case of those obtained from the single point signals. This can be useful for NDTE on ball bearings by extracting the information content from signals measured at the outer ring. In future work, the study will be focused on the propagation of the SAW on a real ball bearing applying the same methods and post processing techniques to extract information related to the integrity of the ball bearing.

**Conflicts of Interest:** The authors declare no conflict of interest.

**Acknowledgement:** This work is supported and funded by CY Cergy Paris University.

**Author contributions:**

Aziz Bouzzit: Writing - Original Draft, Software, Data Curation

Loïc Martinez: Writing - Review & Editing, Validation, Supervision, Data Curation

Andres Arciniegas: Writing - Review & Editing, Validation, Supervision

Salah-Eddine Hebaz: Writing - Review & Editing, Validation, Supervision

Nicolas Wilkie Chancellier: Writing - Review & Editing, Validation, Supervision, Project administration

**References**

- [1] Lamb H. On the vibrations of an elastic sphere. *Proceedings of the London Mathematical Society* 1881;s1-13:189–212. <https://doi.org/10.1112/plms/s1-13.1.189>.
- [2] Gilbert F. Excitation of the Normal Modes of the Earth by Earthquake Sources. *Geophys J Int* 1971;22:223–6. <https://doi.org/10.1111/j.1365-246X.1971.tb03593.x>.
- [3] Royer D, Dieulesaint E, Jia X, Shui Y. Optical generation and detection of surface acoustic waves on a sphere. *Appl Phys Lett* 1988;52:706–8. <https://doi.org/10.1063/1.99353>.
- [4] Tsukahara Y, Nakaso N, Cho H, Yamanaka K. Observation of diffraction-free propagation of surface acoustic waves around a homogeneous isotropic solid sphere. *Appl Phys Lett* 2000;77:2926–8. <https://doi.org/10.1063/1.1322056>.
- [5] Yamanaka K, Cho H, Tsukahara Y. Precise velocity measurement of surface acoustic waves on a bearing ball. *Appl Phys Lett* 2000;76:2797–9. <https://doi.org/10.1063/1.126481>.
- [6] Clorennec D, Royer D. Investigation of surface acoustic wave propagation on a sphere using laser ultrasonics. *Appl Phys Lett* 2004;85:2435–7. <https://doi.org/10.1063/1.1791331>.
- [7] Yamanaka K, Singh KJ, Iwata N, Abe T, Akao S, Tsukahara Y, et al. Acoustic dispersion in a ball-shaped surface acoustic wave device. *Appl Phys Lett* 2007;90:214105. <https://doi.org/10.1063/1.2741606>.

- [8] Martinez L, Wilkie-Chancellor N, Glorieux C, Sarens B, Caplain E. Transient space-time surface waves characterization using Gabor analysis. *J Phys Conf Ser* 2009;195:012009. <https://doi.org/10.1088/1742-6596/195/1/012009>.
- [9] Royer D, Clorennec D. Theoretical and Experimental Investigation of Rayleigh Waves on Spherical and Cylindrical Surfaces. 2008.
- [10] Otsuka PH, Matsuda O, Tomoda M, Wright OB. Interferometric imaging of surface acoustic waves on a glass sphere. *J Appl Phys* 2010;108. <https://doi.org/10.1063/1.3517076>.
- [11] van Damme B, Spadoni A. Frequency-dependent, near-pole behavior of acoustic surface waves on a solid sphere. *Mech Res Commun* 2014;60:40–4. <https://doi.org/10.1016/j.mechrescom.2014.05.002>.
- [12] Ma X, Tang X, Wang Z, Gao D, Tang Y. Theoretical and experimental investigation of surface acoustic wave propagation on a hollow spherical shell using laser ultrasound. *AIP Adv* 2016;6:125036. <https://doi.org/10.1063/1.4972283>.
- [13] Chen S, Sabato A, Niezrecki C. Estimation of the Dynamic Focused Ultrasound Radiation Force Generated by an Ultrasonic Transducer, 2017, p. 15–22. [https://doi.org/10.1007/978-3-319-54987-3\\_3](https://doi.org/10.1007/978-3-319-54987-3_3).
- [14] Giurgiutiu V. Chapter 7 - Piezoelectric Wafer Active Sensors – PWAS Transducers. In: Giurgiutiu V, editor. *Structural Health Monitoring with Piezoelectric Wafer Active Sensors (Second Edition)*. Second Edition, Oxford: Academic Press; 2014, p. 357–94. <https://doi.org/https://doi.org/10.1016/B978-0-12-418691-0.00007-1>.
- [15] Alleyne D, Cawley P. A two-dimensional Fourier transform method for the measurement of propagating multimode signals. *J Acoust Soc Am* 1991;89:1159–68. <https://doi.org/10.1121/1.400530>.
- [16] Sachse W, Pao Y. On the determination of phase and group velocities of dispersive waves in solids. *J Appl Phys* 1978;49:4320–7. <https://doi.org/10.1063/1.325484>.
- [17] Pialucha T, Guyott CCH, Cawley P. Amplitude spectrum method for the measurement of phase velocity. *Ultrasonics* 1989;27:270–9. [https://doi.org/10.1016/0041-624X\(89\)90068-1](https://doi.org/10.1016/0041-624X(89)90068-1).
- [18] Flax L, Dragonette LR, Überall H. Theory of elastic resonance excitation by sound scattering. *J Acoust Soc Am* 1978;63:723–31. <https://doi.org/10.1121/1.381780>.
- [19] Lord Rayleigh. *Lord Rayleigh\_On Waves Propagated along the Plane Surface of an Elastic Solid\_1885*. London Mathematical Society 1885. <https://doi.org/https://doi.org/10.1112/plms/s1-17.1.4>.